General Disclaimer

One or more of the Following Statements may affect this Document

- This document has been reproduced from the best copy furnished by the organizational source. It is being released in the interest of making available as much information as possible.

- This document may contain data, which exceeds the sheet parameters. It was furnished in this condition by the organizational source and is the best copy available.

- This document may contain tone-on-tone or color graphs, charts and/or pictures, which have been reproduced in black and white.

- This document is paginated as submitted by the original source.

- Portions of this document are not fully legible due to the historical nature of some of the material. However, it is the best reproduction available from the original submission.

SEMIANNUAL PROGRESS REPORT

(March 1975 - August 1975)

Grant No: NGR-09-005-063

Title: Magnetosphere of Mercury

Technical Monitor: Dr. E. R. Schmerling, Code SG

Principal Investigator: Y. C. Whang, Professor
Catholic University of America
Washington, D. C. 20064

The third encounter of Mariner 10 with Mercury occured on March 16, 1975. The magnetic field data obtained during this flyby confirmed that Mercury possesses a modest intrinsic magnetic field sufficient to deflect the solar wind flow. Our present research is to study the model magnetosphere of Mercury using Mariner 10 data.

Because the planet Mercury occupies a very large fraction of the volume of the magnetosphere, the observed magnetic field data from Mariner 10 represents the vector sum of the planetary intrinsic field, the Chapman-Ferraro field due to magnetopause current and the tail field due to current in the tail sheet. We use the image-dipole method to represent the model magnetosphere.

A new feature identified from our model study is the crossing of the Mariner 10 spacecraft over the tail sheet of Mercury at 2047 UT March 29, 1974 during the first encounter as shown in Figure 1. The thickness of the tail sheet is approximately 100 km at the crossing. A summary of the magnetospheric field calculated from our model is shown in Figure 2, which shows the field lines in the noon-midnight meridian plane. All planetary field lines are confined inside a magnetopause. The size of the model magnetosphere also agrees with the magnetopause crossings directly observed from Mariner 10. The magnitude of the magnetic field at the stagnation point is consistent with the observed solar wind condition.

(NASA-CR-143429) MAGNETOSPHERE OF MERCURY Semiannual Progress Report, Mar. - Aug. 1975 (Catholic Univ. of America) 26 p HC $3.75 CSCL 03B

N75-31985

Unclas
G3/91 35222

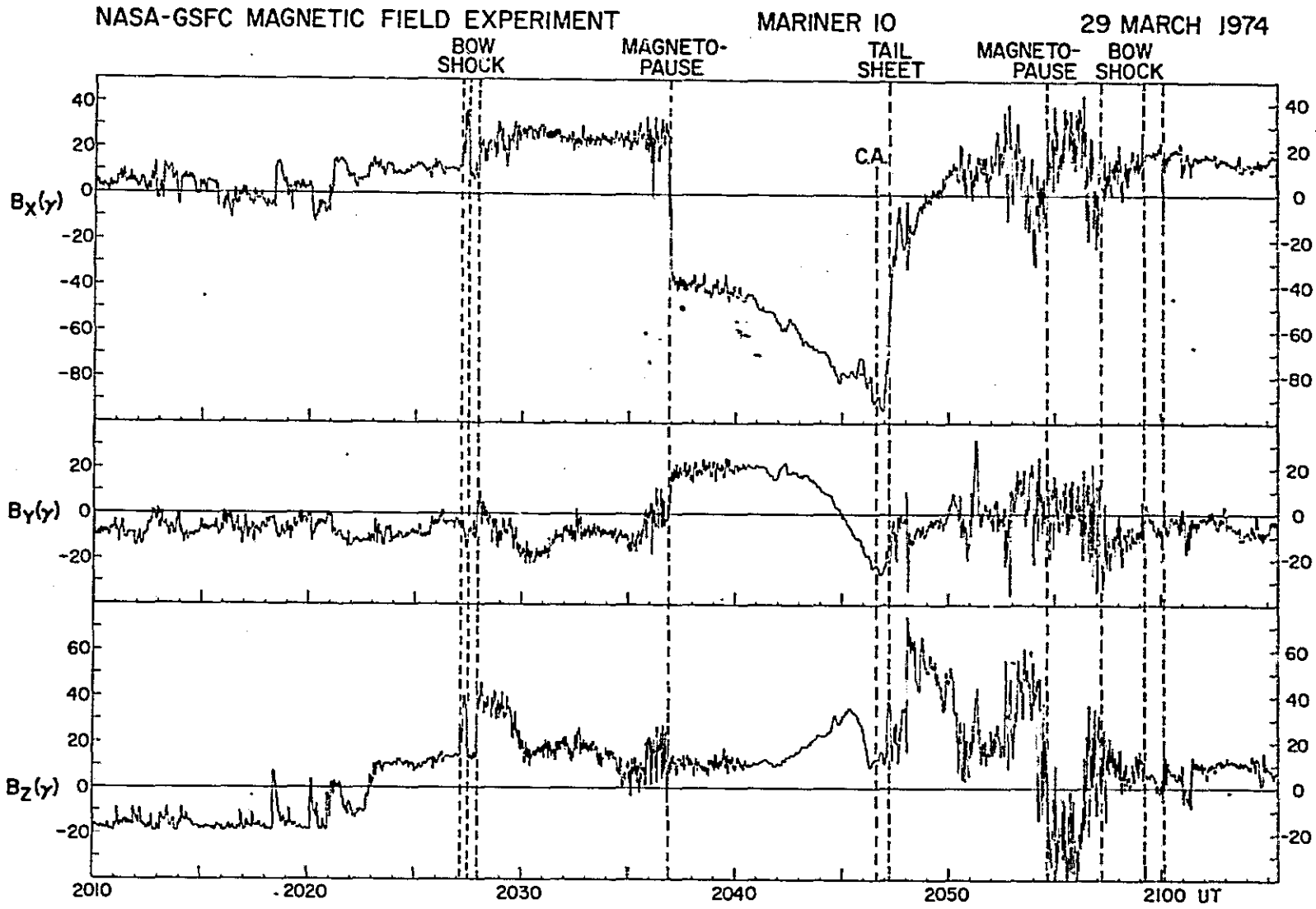
NASA-GSFC MAGNETIC FIELD EXPERIMENT
MARINER 10
29 MARCH 1974
BOW SHOCK
MAGNETO-PAUSE
TAIL SHEET
MAGNETO-PAUSE
BOW SHOCK
C.A.
$B_X(\gamma)$
$B_Y(\gamma)$
$B_Z(\gamma)$
40
20
0
-20
-40
-60
-80
60
2010
2020
2030
2040
2050
2100 UT

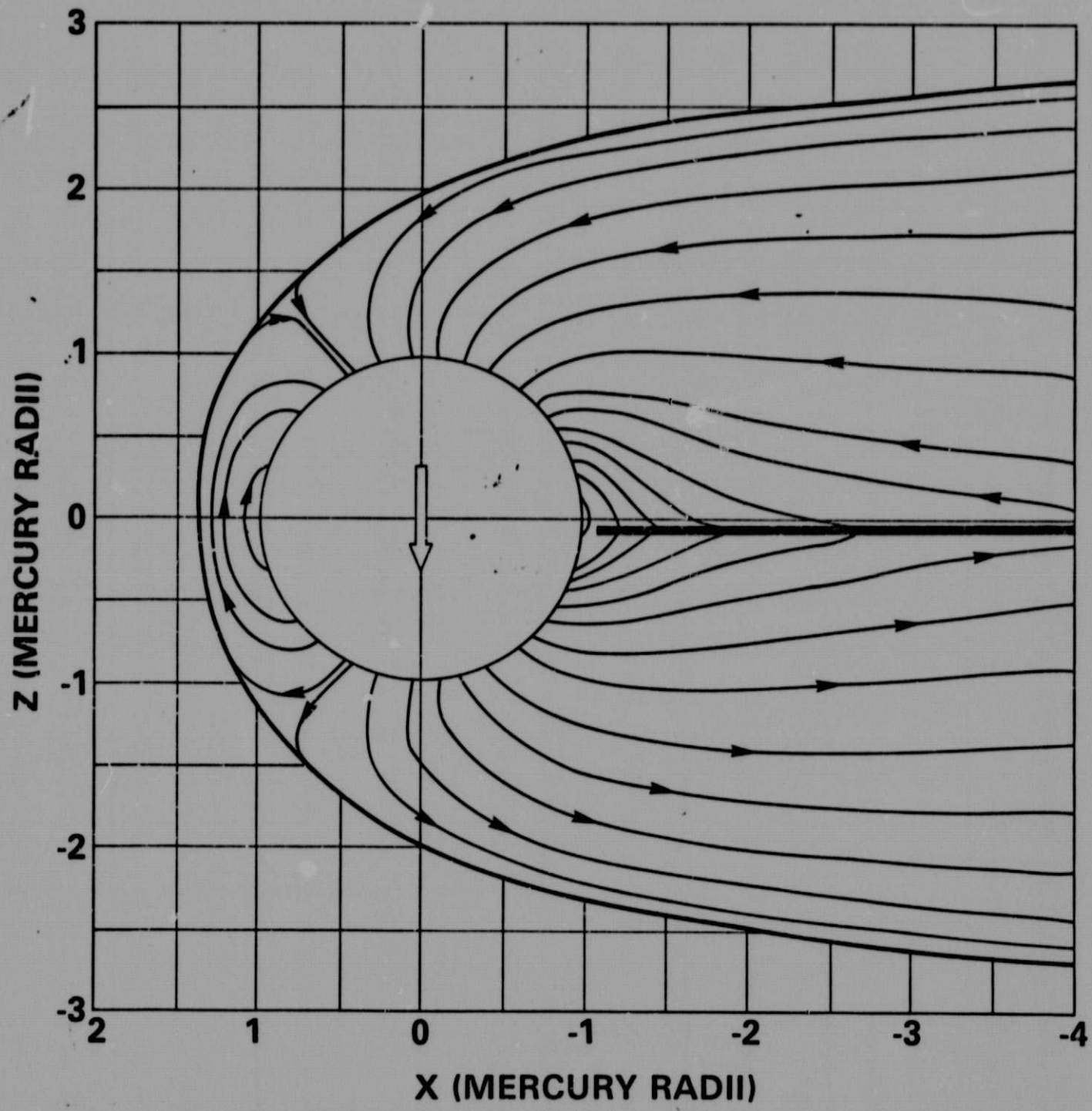

Figure 2

Publications (copies of these papers are enclosed).

(1) Y. C. Whang, N. F. Ness, K. W. Behannon and R. P. Lepping, "Magnetospheric Magnetic Field of Mercury", EOS, 56, 619 (Sept. 1975).

(2) N. F. Ness, K. W. Behannon, R. P. Lepping, and Y. C. Whang, "Magnetic Field of Mercury Confirmed", Nature, 255, 205 (May 15, 1975).

(3) N. F. Ness, K. W. Behannon, R. P. Lepping, and Y. C. Whang, "The Magnetic Field of Mercury", JGR, 80, 2708 (July 1975).

Papers presented at conferences by Y. C. Whang

(1) "Magnetospheric Field of Mercury", AGU Topical Conference on Quantitative Magnetospheric Models", La Jolla, CA, May 6-8, 1975.

(2) "Model Magnetosphere of Mercury Deduced from Mariner 10 Data", AGU Annual Meeting, Washington, D. C., (June 16-19, 1975).

(3) "Magnetohydrodynamic Expansion of the Solar Wind", IAGA Meeting, Grenoble, France, (Aug. 25-Sept. 3, 1975).

MAGNETOSPHERIC MAGNETIC FIELD OF MERCURY

Y.C. Whang (Catholic University of America, Washington, D.C. 20064)
N. F. Ness, K. W. Behannon, R. P. Lepping (Laboratory for Extraterrestrial Physics, NASA-Goddard Space Flight Center, Greenbelt, Maryland 20771)

The first encounter of Mariner 10 with Mercury (Mercury I) occurred on 29 March 1974. The magnetic field measurements during the Mercury I encounter unexpectedly revealed that the planet Mercury has a significant intrinsic magnetic field. The interaction of the solar wind with Mercury is Earth-like. The planetary magnetic field is compressed to form a magnetosphere, and a detached bow shock is formed upstream of the planet.

The second encounter of Mariner 10 with Mercury took place on 21 September 1974. The targeting strategy of the second encounter was to provide optimum imaging coverage of the south polar region, and the spacecraft passed the planet on the sunward side at too great a distance to permit observations inside the planet's bow shock. The third, and last, encounter took place on 16 March 1974, at which time the spacecraft flew on a near collision course, the distance from the planetary surface at closest approach being approximately 330 km. Magnetic field data from the Mercury III encounter provided unequivocal evidence that there exists an intrinsic planetary magnetic field, and yielded further data on the nature of its interaction with the solar wind.

This paper presents a model study of the magnetospheric magnetic field of Mercury using Mercury I data. The planet Mercury occupies a very large fraction of the volume of the magnetosphere. A substantial part of the observed magnetic field data during the Mercury I encounter is due to external sources: the magnetopause current and the tail sheet current. We adopt the image-dipole method of Hones and Taylor to study the model magnetosphere. The available data set being very limited essentially restricts us to the choice of a simple model. We assume that the

intrinsic dipole M is normal to the equatorial plane at the center of the planet; an image dipole $M_i = GM$ is placed at (x_i, o, o) in the antisolar direction, and a tail current sheet of finite thickness is parallel to the equatorial plane on the dark side. We require that the magnetic field is divergence-free and curl-free everywhere inside the magnetosphere except at the tail current sheet, and that at the boundary all field lines are tangential to a magnetopause-like surface.

In the absence of other fields, the tail field may be represented by a new analytical solution

$$B_x = -r_t^{-1/2} \sin \frac{\omega}{2} \; F$$

and

$$B_z = r_t^{-1/2} \cos \frac{\omega}{2} \; F$$

in the region: $-\pi < \omega < \pi$ with a branch cut at $\omega = \pm\pi$

Here

$$r_t = \left[(x-x_t)^2 + (z-z_t)^2 \right]^{1/2}$$

and

$$\omega = \tan^{-1} \left(\frac{z-z_t}{x-x_t} \right)$$

F is real and the line (x_t, z_t) is the inner edge of a tail current sheet. We may write this basic solution of the tail field as a function of a complex variable

$$B_z + iB_x = (\zeta - \zeta_t)^{-1/2} \; F$$

where $\zeta = x + iz$. Then a general solution of the tail field may be represented by the integral of the basic solution

$$\iint F(\zeta_t) (\zeta - \zeta_t)^{-1/2} \, dx_t dz_t$$

over a tail sheet: $-\infty < x_t < a \; (<o)$ and $-d/2 < z_t < d/2$. This insures that the integral remains divergence-free and curl-free everywhere except at the tail current sheet of finite thickness. A special solution with

$$F(\zeta_t) = B_t x^{-2}$$

is used in the present model study for which the integral for the tail field, its potential and the field lines can all

be expressed in an analytical closed form.

The Mercury I magnetic field data during the interval from 2038 to 2047 UT and from 2049 to 2052 UT are used to describe a representative magnetospheric field of the planet. The result of this study qualitatively explains many important observed features. The model magnetic field is represented by the dashed curves in Figure I and the three components

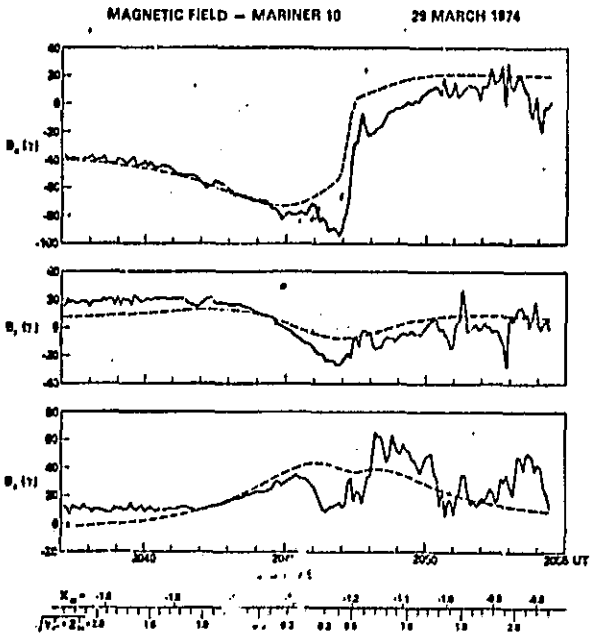

Figure I

of the observed field are represented by solid curves. From this study, we can identify that at 2047 UT the spacecraft flew past the tail sheet of Mercury, and that the thickness d of the tail sheet is approximately 100 km at the crossing point.

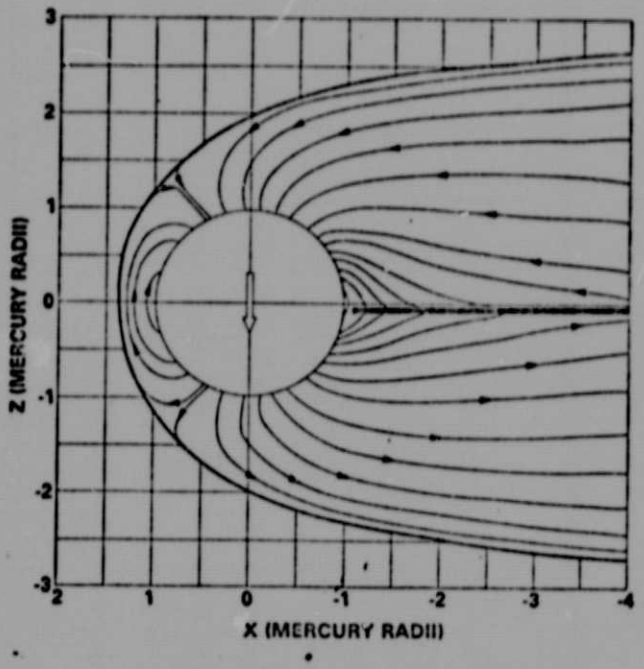

Figure 2

Figure 2 shows the magnetospheric field lines in the noon-midnight meridian plane. All planetary field lines are confined inside a magnetopause and the size of the model magnetosphere agrees with the magnetopause crossings directly observed from Mercury I data. The model magnetosphere has nearly circular cross-sections and the magnitude of the magnetic field at the stagnation point is also consistent with the solar wind condition directly observed from Mercury I.

Acknowledgements The work at the Catholic University of America was supported by the National Aeronautics and Spacc Administration under Grant NGR-09-005-063.

MAGNETIC FIELD OF MERCURY CONFIRMED

N. F. Ness, K. W. Behannon
R. P. Lepping and Y. C. Whang*
Laboratory for Extraterrestrial Physics
NASA-Goddard Space Flight Center
Greenbelt, Maryland 20771 USA

*The Catholic University of America
Washington, D. C. 20064 USA

On 16 March 1975, the USA Spacecraft Mariner 10 achieved its third and final encounter with the planet Mercury. This unique and fortuitous event occurred because the heliocentric orbital period of Mariner 10 was 176 days, exactly twice that of the orbital period of Mercury, 88 days. The principal objective of the third flyby was to confirm or reject the suggestion from the first flyby on 29 March 1974 that Mercury may possess a modest intrinsic magnetic field sufficient to deflect the solar wind flow[1-2]. The quantitative analysis[3] of the Mercury I data yielded an estimate of the planetary magnetic dipole moment equal to 5.1×10^{22} Gauss cm^3 and oriented 7° from the orbit normal. The spacecraft was severely limited in its ability to function properly since Mercury I due to various technical failures. However, a dedicated effort by the spacecraft engineering team at NASA/JPL achieved the desired objective at Mercury III of a very close darkside pass at the planet. This letter presents preliminary results from the NASA/GSFC magnetometer instrumentation on Mariner 10.

The flyby trajectory is shown in planetary centered solar ecliptic coordinates in Figure 1. This is a preliminary trajectory and will be

updated with post encounter tracking observations when they have been analyzed. The nominal miss distance at closest approach was approximately 323±8 km. For comparison, also shown in Figure 1 is the trajectory at Mercury I encounter, for which the closest approach miss distance was = 704 km. In the right panel, showing the view from the Sun, the much higher latitude pass of the spacecraft during Mercury III is well illustrated. This closer and more poleward targeting was chosen so as to yield magnetic field measurements which would provide unequivocal evidence regarding the nature of the planetary magnetic field at Mercury. The Mercury I results were consistent with a reduced scale model of the solar wind interaction with the terrestrial magnetic field, in which the planetary field is compressed by the solar wind flow, which itself is deflected around the planet, and a detached bow shock wave forms. As a result, the field is then confined to a region of space close to the planet on the Sunward side and extended to form a magnetic tail on the nightside.

Based upon the observations and analysis at Mercury I and assuming similar conditions of solar wind momentum flux at Mercury III, predictions were made of the locations where the characteristic bow shock and magnetopause boundaries would be observed. The position of these boundary surfaces is presented in the left panel of Figure 1. Since the rotation period of the planet is uniquely coupled to its orbital period, in the ratio 2:3, the "phase" of the planet relative to the planet-Sun line at successive encounters was identical.

The observed positions of the bow shock and magnetopause during Mercury III are also illustrated in Figure 1. They show excellent

agreement with the model boundaries, which used a scaling of the magnetic moment of Mercury equal to 7×10^{-4} that of the Earth's dipole moment. In the case of the solar wind flux impinging normal to a dipole field, a theoretical study[4] has yielded the relationship $\frac{R_{mp}}{R_p} = 1.07 \left[\frac{B_o^2}{4\pi nmV^2}\right]^{1/6}$

where R_{mp}/R_p = the normalized radius of the stagnation point distance of the magnetopause, B_o = equatorial dipole field intensity, and nmV^2 = solar wind momentum flux (where n = number density, m = mass of proton and V = velocity of solar wind). The distance to the magnetopause, as measured by R_{mp} is thus weakly dependent upon solar wind momentum flux and hence even if variations of $\pm 60\%$ in the solar wind flux occur, they would alter the position of the characteristic bow shock and magnetopause boundaries by only $\pm 10\%$.

The magnetic field measurements were accomplished with a dual magnetometer[5] system which sampled the vector magnetic field 25 times each second, with a precision of $\pm .125\gamma$ for each orthogonal component. These data are to be considered preliminary in that they are accurate to $\pm 1\text{-}2\gamma$ or $\pm 1\%$, which ever is larger, because they are derived from quick look data provided in near real time by JPL. Six second averages of the observed magnetic field throughout the encounter period are shown in Figure 2. The occurrence of the well developed bow shock and magnetopause boundaries are indicated and readily identified by a magnitude and/or directional change as well as in the Pythagorean mean fluctuation characteristic, RMS. The maximum magnitude of the field is 400γ, 4 times larger than that observed at Mercury I encounter and 20 times larger than the interplanetary field, which is close to 20γ. This large value precludes any reasonable possibility that the magnetic barrier to solar wind

flow is associated with a complex induction process occurring at the planet. The direction of the magnetic field, as measured by latitude θ and longitude ϕ, is primarily towards the Sun (and planet) with gradual changes along the trajectory within the magnetosphere boundaries. This orientation is opposite to that observed at Mercury I encounter but is perfectly consistent with the model of a Mercurian magnetosphere[6] in which the planetary field is represented by a centered dipole normal to the solar wind flow and which is then highly distorted by magnetopause currents.

A preliminary spherical harmonic analysis of the data within the magnetosphere has been conducted using the available trajectory. The analysis assumes a centered planetary dipole field, i.e., harmonic order $N = 1$, as well as external field sources described by harmonic terms up to order $N = 2$. The preliminary least-squares fit yields a residual of 7γ with the deduced parameters for the planetary dipole listed in Table I. These are compared with those values derived from Mercury I and are seen to be in remarkably good agreement, considering the preliminary nature of these results. The magnitude of the dipole moment is the same within 10% and its direction only 24° from that derived earlier. The uncertainty associated with the present analysis precludes attributing any significance to these small differences.

In summary, the observations at the third encounter with Mercury by the NASA/GSFC magnetic field experiment have dramatically confirmed the earlier tentative conclusion that Mercury possesses a modest magnetic field intrinsic to the planet. The origin of this magnetic field is at present uncertain. It may be associated with remanent magnetization of portions of the planet, i.e., material presently below its Curie point,

or it may be due to an active dynamo in the presumably large iron/nickel core. It is difficult to construct a plausible sequence of events leading to the model in which the Mercurian magnetic field is due to remanent magnetization. Thus, we conclude tentatively that these observations of an intrinsic magnetic field require the existence of an active dynamo mechanism in the interior of the planet. Future detailed and final studies of the Mercury III encounter results and intercomparison with those from Mercury I encounter, as well as considerations of possible interior structures, should yield significant insight into the present physical state of Mercury.

We express sincere appreciation to Dr. James Dunne, JPL Project Scientist on Mariner 10, and the JPL spacecraft team for their outstanding effort in achieving the third encounter. We also appreciate the special efforts of D. H. Howell, F. W. Ottens and R. E. Thompson of the NASA/GSFC for their special efforts and prompt analysis of these data

References

1. Ness, N. F., Behannon, K. W., Lepping, R. P., and Whang, Y. C., Science, 185, 151 (1974).
2. Ogilvie, K. W., et al., ibid, pg. 145.
3. Ness, N. F., Behannon, K. W., Lepping, R. P., and Whang, Y. C., J. Geophys. Res., 80, in press (1975).
4. Choe, J. T., Beard, D. B., and Sullivan, E. C., Planet. Space Sci., 21, 485 (1973).
5. Ness, N. F., Behannon, K. W., Lepping, R. P., and Schatten, K. W., J. Geophys. Res., 76, 3564 (1971).
6. Whang, Y. C., and Ness, N. F., J. Geophys. Res., 80, submitted (1975).

Table I

Comparison of Planetary Dipole Moments Obtained by Spherical Harmonic Analysis of Magnetic Field Data

	Mercury I	Mercury III
	29 March 1975	16 March 1975
Dipole Moment (Gauss cm^3)	5.1×10^{22}	$4.8(\pm.5) \times 10^{22}$
	$(350\gamma\ R_m^3)$	$(330 \pm 30\gamma\ R_m^3$
Latitude (ME coordinates)	-80°	$-76^\circ \pm 5^\circ$
Longitude (ME coordinates)	285°	$90 \pm 30^\circ$
Root Mean Square Residual	0.9γ	7γ
Comment	(Quiet Data Only)	(Preliminary but entire data set)

List of Figures

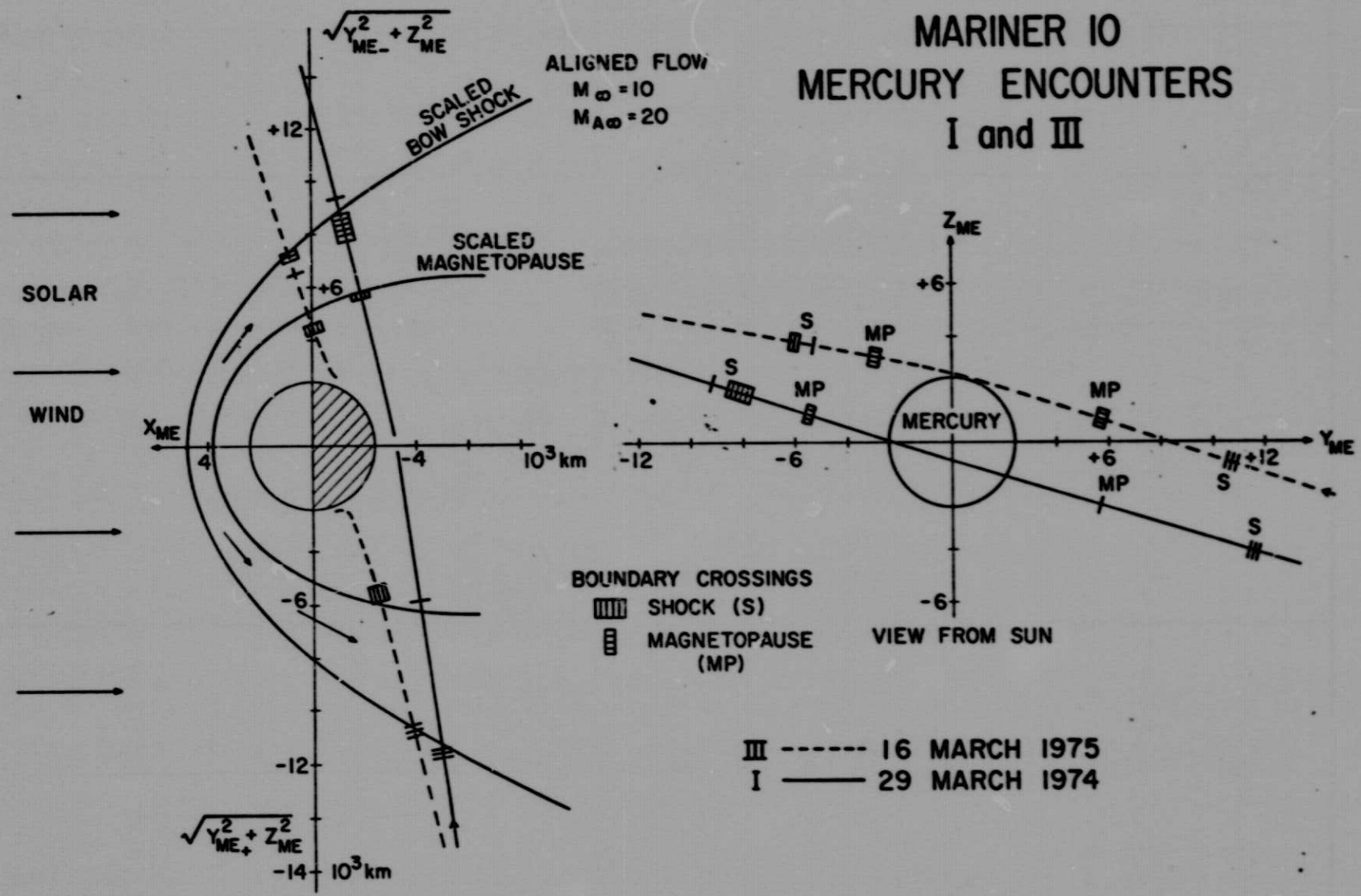
MARINER 10
MERCURY ENCOUNTERS
I and III
ALIGNED FLOW
$M_\infty = 10$
$M_{A\infty} = 20$
SCALED BOW SHOCK
SCALED MAGNETOPAUSE
SOLAR WIND
$\sqrt{Y_{ME-}^2 + Z_{ME}^2}$
$\sqrt{Y_{ME+}^2 + Z_{ME}^2}$
X_{ME}
Z_{ME}
Y_{ME}
+12
+6
-6
-12
-14
4
-4
10^3 km
S
MP
MERCURY
BOUNDARY CROSSINGS
SHOCK (S)
MAGNETOPAUSE (MP)
VIEW FROM SUN
III ------ 16 MARCH 1975
I —— 29 MARCH 1974

Figure 1

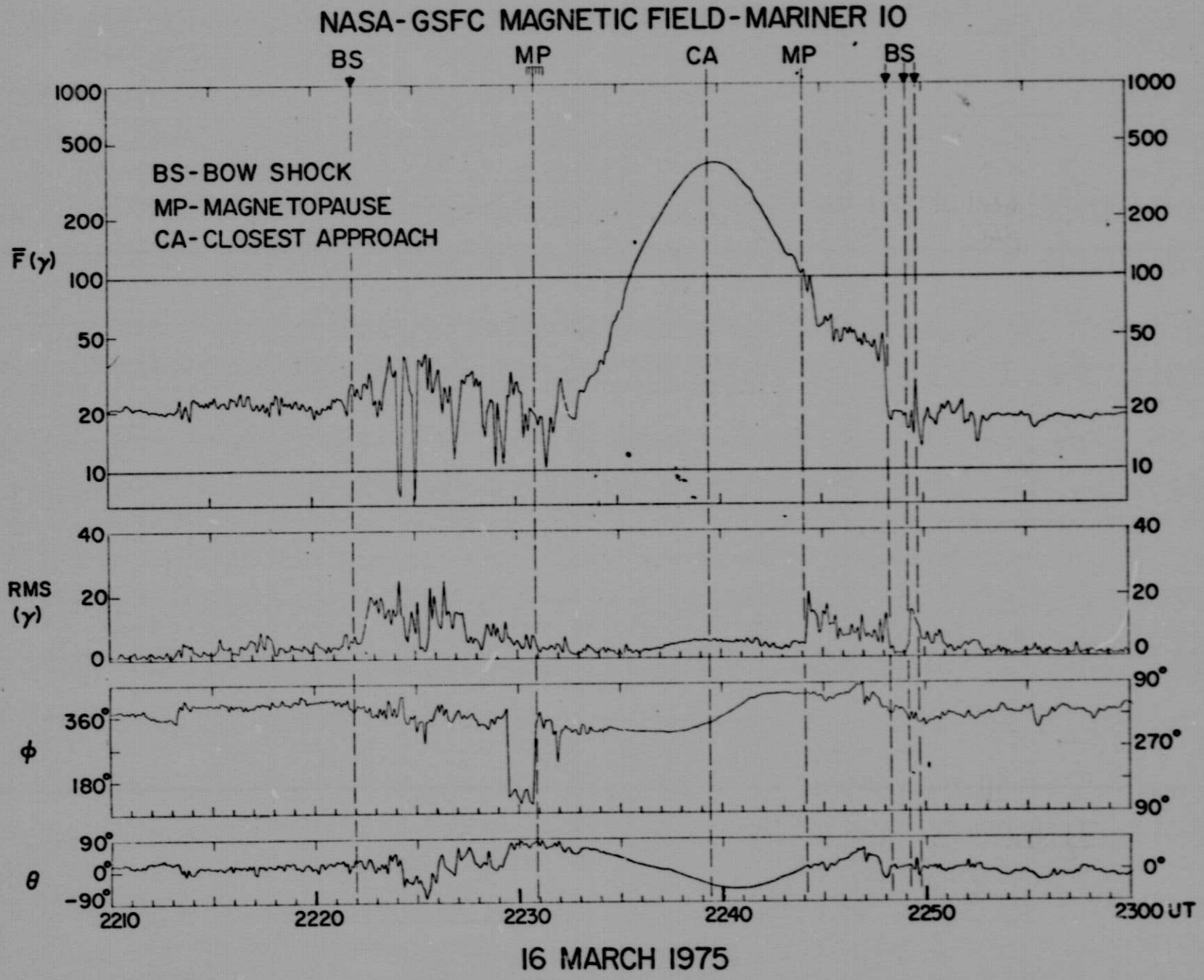
NASA-GSFC MAGNETIC FIELD-MARINER 10
BS
MP
CA
MP
BS
BS-BOW SHOCK
MP-MAGNETOPAUSE
CA-CLOSEST APPROACH
F̄(γ)
1000
500
200
100
50
20
10
RMS (γ)
40
20
0
φ
360°
180°
90°
270°
θ
90°
0°
-90°
2210
2220
2230
2240
2250
2300 UT
16 MARCH 1975

Figure 2

The Magnetic Field of Mercury, 1

N. F. NESS, K. W. BEHANNON, AND R. P. LEPPING

Laboratory for Extraterrestrial Physics, NASA Goddard Space Flight Center Greenbelt, Maryland 20771

Y. C. WHANG

Catholic University, Washington, D. C. 20064

An updated analysis and interpretation are presented of the magnetic field observations obtained during the Mariner 10 encounter with the planet Mercury on March 29, 1974. The combination of data relating to position of the detached bow shock wave and magnetopause and the geometry and magnitude of the magnetic field within the magnetospherelike region surrounding Mercury lead to the conclusion that an internal planetary field exists with dipole moment approximately 5.1×10^{22} G cm^3. The limited data set precludes quantitative determination of an intrinsic field more complex than a centered dipole. The dipole axis has a polarity sense similar to that of earth and is tilted 7° from the normal to Mercury's orbital plane. The magnetic field observations reveal a significant distortion of the modest Hermean field (350 γ at the equator) by the solar wind flow and the formation of a magnetic tail and neutral sheet which begins close to the planet on the night side. Presently, an active dynamo mechanism in the planetary interior appears to be favored in the interpretation of the field origin, although fossil remanent magnetization cannot be excluded. The composite data set is not consistent with a complex induction process driven by the solar wind flow.

INTRODUCTION

The first in situ measurements of the solar wind interaction with the planet Mercury and its magnetic field were performed by the Mariner 10 spacecraft on March 29, 1974. A preliminary report [*Ness et al.*, 1974*b*] presented the initial results of the analysis of data obtained from the dual magnetometer experiment. The unexpected observation of a very well developed strong detached bow shock wave was interpreted as being due to the existence of a modest magnetospherelike region associated with an intrinsic magnetic field of the planet. Simultaneous measurements of the low-energy electron flux ($13.4 < E_e < 687$ eV) by *Ogilvie et al.* [1974] provided strong correlative evidence for this interpretation. In addition, intense bursts of higher-energy electrons ($E_e > 170$ keV) and protons ($E_p > 500$ keV) were reported by the charged particle telescope experiment [*Simpson et al.*, 1974] as occurring in a region of space corresponding to the magnetosphere and magnetosheath following the closest approach to Mercury of Mariner 10.

The previous report by *Ness et al.* [1974*b*] also discussed the possibility of a complex induction mode, due to solar wind transport of the interplanetary field past the planet, leading to the set of observations obtained. A review of the arguments presented then against the induction mode hypothesis does not indicate any need at the present time for further consideration. The combination of factors relating to the geometry and positions of the bow shock and magnetopause, which implies a scale size of solar wind interaction larger than the planet, and both the geometry and the magnitude of the magnetic field within the magnetospherelike region are found to be inconsistent with present models of such planetary interactions. The lack of evidence for any appreciable atmosphere or ionosphere [*Broadfoot et al.*, 1974; *Howard et al.*, 1974] suggests that the interaction is unlike that at Venus, wherein a substantial atmosphere-ionosphere is responsible for the deflection of the solar wind flow and the development of the detached bow shock wave [*Bridge et al.*, 1974; *Ness et al.*, 1974*a*].

A unique feature of the Mariner 10 heliocentric orbit is that following the gravity assist at Venus, the orbital period is exactly twice Mercury's period, so that on September 21, 1974, a second encounter with the planet occurred. The targeting strategy for that encounter was biased to provide optimum imaging coverage of the south polar regions, and so the spacecraft did not approach sufficiently close to the planet (minimum distance $\approx 5 \times 10^4$ km) to observe directly the magnetic field of the planet and/or any effects associated with the solar wind interaction. A third encounter will occur on March 16, 1975, and appropriate targeting plus successful spacecraft performance should permit additional observations of the magnetic field environment and solar wind interaction with the planet Mercury.

It is the purpose of this report to present a brief review of the magnetic field observations and the updated final result of the quantitative analysis of the first encounter data yielding an estimate of the intrinsic magnetic field of the planet Mercury.

MAGNETIC FIELD OBSERVATIONS

Detailed data obtained near the first Mercury encounter are presented in Figure 1. Individual data points used in this figure represent a reconstituted vector magnetic field obtained from 1.2-s component averages by utilizing the 25-Hz vector magnetic field sampling rate of the instrument. Details regarding the accuracy of magnetic field measurements obtained with the dual magnetometer system on this, its first flight, have already been presented [*Ness et al.*, 1974*a*]. The data in Figure 1 illustrate very clearly the important features of the magnetic field measurements. A multiple crossing of the bow shock occurs between 2027 and 2028 UT on March 29, 1974. It is well identified both by the abrupt increase in average field magnitude and by the increase in the fluctuating magnetic field, as measured by the rms parameter.

The magnetopause is well distinguished by the abrupt direc-

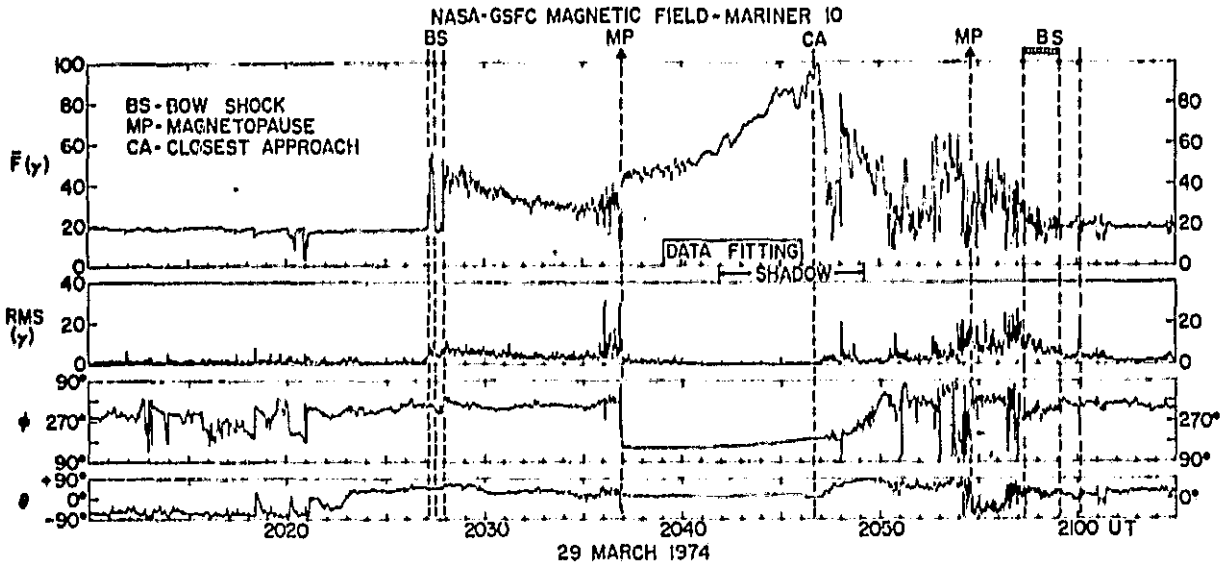

Fig. 1. Magnetic field data averages for 1.2-s periods during encounter in spacecraft-centered solar ecliptic coordinates. The latitude of the reconstituted vector is represented by θ and longitude by ϕ, the field intensity by F, while rms represents the Pythagorean mean of the X, Y, Z component root mean square deviations. The X axis is directed to the sun, the Z axis to north ecliptic pole, and the Y axis completes the right-handed coordinate system.

tional change in the magnetic field, noted primarily in the ϕ curve, but is also reflected in the abrupt termination of high frequency fluctuations measured by the rms parameter. The average field magnitude is observed to increase across the magnetopause. Between this boundary crossing and the closest approach the magnetic field is seen to be rather steady in direction, especially with respect to higher frequency fluctuations. It is noted that between 2040 and 2046 UT the magnetic field fluctuations are substantially less than those in the magnetosheath and even markedly smaller than those in the interplanetary medium. Small-amplitude, $< 5\ \gamma$, and longer-period fluctuations, periods greater than a few seconds, are observed in this portion of the magnetosphere.

Following closest approach, abrupt and large variations of the magnetic field are observed. It is important to note in this data presentation that although the field magnitude varies by up to 50% from its average value throughout the data set up to the outbound magnetopause crossing, the general direction of the magnetic field does not change. In other words, an average direction of the magnetic field exists during this period of time which is not destroyed by the large-amplitude fluctuations of the magnetic field. The rapid time variations of the magnetic field following closest approach and the associated electron flux measurements have been interpreted in terms of a substorm which disturbed the Hermean magnetosphere in association with a southward turning of the interplanetary magnetic field during the encounter [*Siscoe et al.*, 1975].

The identification of the outbound magnetopause near 2054 UT is based on a large directional change in the magnetic field from a large positive θ to large negative θ. Subsequently, the spacecraft remains in the rather disturbed magnetosheath until the bow shock crossings are observed. The identification of the outbound bow shock crossing is much less distinctive than the inbound shock crossing due to both the disturbed nature of the Hermean magnetosphere at this time and the orientation of the interplanetary magnetic field. As was previously discussed by *Ness et al.* [1974*b*], the contrast is due to the different relative orientations of the interplanetary magnetic field. It was nearly orthogonal to the bow shock surface normal when Mariner 10 was inbound and conversely was rather more parallel outbound.

The data obtained within the magnetopause crossings are presented in a different format in Figure 2. Here 42-s average vector components are plotted in two different planes, as viewed from the sun along the $-X$ axis and as projected on a plane parallel to the ecliptic. In the lower portion of the figure the traces of a magnetopause and bow shock boundary, scaled for the case of a dipole magnetic moment of Mercury equal to 7×10^{-4} of earth's moment, are included. A few of the vectors representing observations outside the magnetopause, when the spacecraft was within the magnetosheath, are also shown to illustrate the sharp and distinctive change in the field direction which occurs at these boundaries.

The quiet interval of the magnetosphere observations is identified, and there the magnetic field has a directional sense analogous to that of the earth's magnetosphere on the near dark side. In that region of space the magnetic tail is beginning to develop. While the large-scale disturbances of the magnetic field occurring after closest approach are readily evidenced in the lower portion of the figure, the preservation of the magnetic field direction previously referenced is illustrated in the upper portion of the figure, the field being roughly parallel to the $+Z$ axis and positive throughout.

It is instructive to compare these data presentations with Figure 3, which illustrates the general characteristics of the external magnetic fields which result from the solar wind interaction with the geomagnetic field. As the solar wind is deflected around the earth, whose dipole is almost perpendicular to the flow of solar wind, the nominal stagnation point of flow occurs at 10 R_E, and the geomagnetic field is confined to a region of space originally called the Chapman-Ferraro cavity and now known as the magnetosphere. Electrical currents which flow on the surface of the magnetosphere, i.e., in the magnetopause, are responsible for the abrupt change in direction which is characteristically observed in the magnetic field as a spacecraft crosses this surface. On a larger scale these fields extend throughout the magnetosphere with approximately the geometry shown. In addition, the development of the

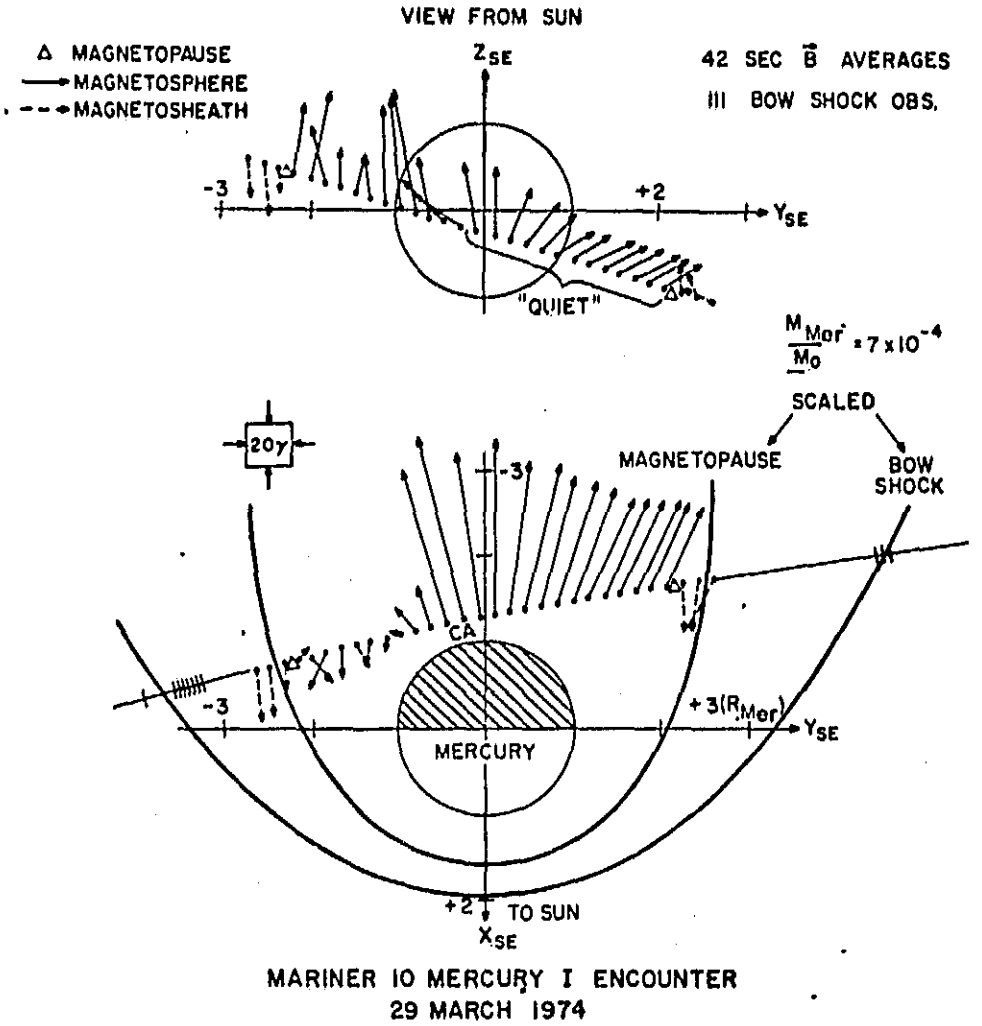

Fig. 2. Observed 42-s average magnetic field vectors superimposed on trajectory of Mariner 10 in X-Z (top) and X-Y (bottom) planes during transit of Hermean magnetosphere. The actual magnetopause crossings are identified, along with the detached bow shock observations. The boundaries represent a best graphical fit obtained by scaling the case of the solar wind interaction with the earth for $M = 7 \times 10^{-4}$ of the earth's magnetic moment; $R_{Mer} = 2439$ km.

geomagnetic tail and embedded neutral sheet is due to a second system of electrical currents whose magnetic field can be described as having an origin associated with the tail of the magnetosphere.

Note that these external fields have a rather specific directional characteristic. Below the plane of the equator and the neutral sheet, which are assumed to be coincident in this figure, the component parallel to the sun-earth line is always directed in an antisolar sense, while above that plane it points sunward. However, the field component parallel to the dipole axis depends upon the observer's position relative to the boundary of the Chapman-Ferraro cavity and to the magnetic tail neutral sheet but is never observed to reverse polarity.

From studies of the earth's magnetosphere it is known that in the immediate vicinity of the neutral sheet a region of significantly weakened magnetic field strength is always measured coincident with the change of the sign of the component parallel to the earth-sun line.

The magnetic field observations by Mariner 10 show a rather good correspondence to the earth's magnetosphere if an appropriate scaling of sizes is taken into account. If the stagnation point of solar wind flow is inferred to be at 1.6 R_{Mer} (Mercury radii), then the scaling yields the results shown in Figure 3. There it is seen that the planet Mercury occupies a very large fraction of the volume of the magnetosphere. Thus, even when measurements are performed relatively close to the surface of the planet, the total field includes a substantial part due to the external sources. This is quite unlike the situation for near earth orbiting spacecraft.

It is this fact, coupled with a very limited data set available in a restricted volume of the magnetosphere sampled by Mariner 10, which limits the ability to analyze the data properly in terms of an intrinsic internal planetary magnetic field. While quantitative models describing the magnetic field in the terrestrial magnetosphere exist, their results are generally sensitive to the choice of parameter values employed when they are in close proximity to either the magnetopause or the neutral sheet. Away from these regions, that is, in the well-developed geomagnetic tail or within 8 R_E, the models are moderately successful in describing the asymmetry of the radiation belts, the polar cap regions, and associated phenomena.

It is not necessary that we attempt to determine a magnetic field representation valid throughout the entire Hermean magnetosphere in order to estimate the intrinsic planetary field. What is needed is to represent the magnetic field

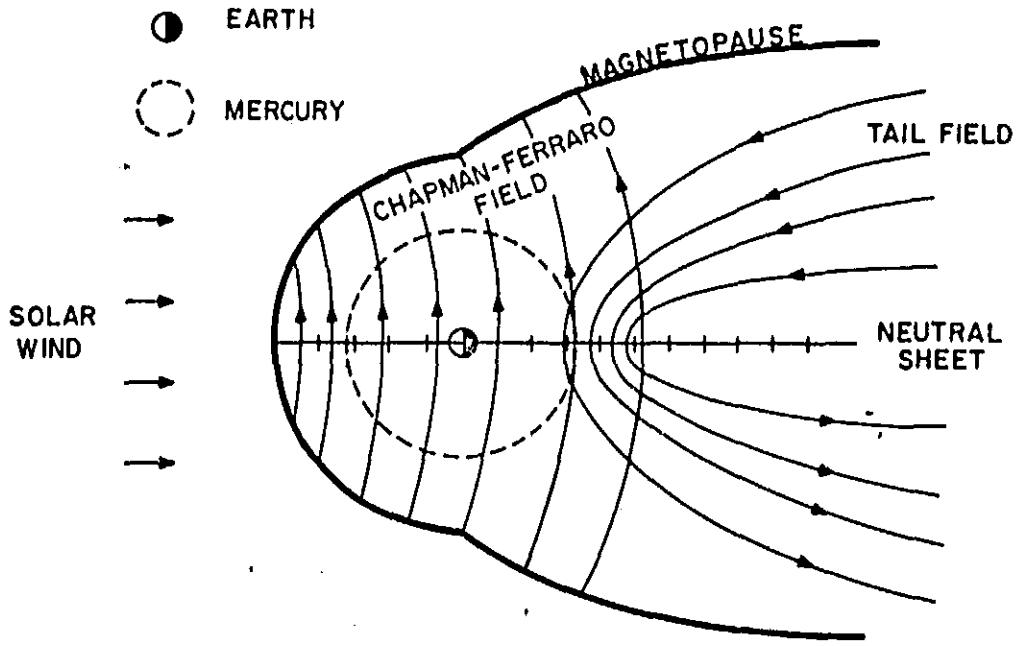

Fig. 3. Sketch in noon-midnight meridian plane of secondary magnetic fields generated by the deflection of solar wind flow around geomagnetic field and extension of polar cap magnetic flux to form magnetic tail. For comparison, the size of Mercury within its magnetosphere is shown.

properly along the trajectory and then to ascertain whether or not the internal field thus obtained provides a consistent description of the Hermean magnetosphere and its interaction with the solar wind. The next section presents such an analysis.

Least Squares Data Fit

In the preliminary report on these results [*Ness et al.*, 1974*b*] the very simplified representation of the magnetic field as being due entirely to an offset tilted magnetic dipole was made, and no external sources of field were considered. By using only quiet interval data, immediately surrounding closest approach, a reasonable data fit was obtained with an rms of $\sim 10\ \gamma$ based upon an offset dipole of magnitude 3.3×10^{22} G cm^3, oriented at latitude $-70°$ and longitude 209°. This moment was 40% smaller than that inferred from the position of the bow shock and magnetopause, 5.6×10^{22} G cm^3. It was compensated by the moderately large offset: 0.47 R_{Mer} at a latitude $\theta = +17°$ and longitude $\phi = 62°$.

Unfortunately, the magnetic field data set which is available for analysis is incomplete in a mathematical sense. The unique determination of the characteristics of that portion of the observed magnetic field which can be ascribed to the interior of the planet demands a set of vector observations over a simple surface enclosing the planet, for example, on a sphere. In the absence of such a data set it is necessary to make additional assumptions regarding the nature of the magnetic field characteristics in order to estimate the interior field.

Since there is no evidence for the existence of a permanently trapped radiation belt [*Simpson et al.*, 1974] nor an ionosphere [*Howard et al.*, 1974], we assume that the region of space between the surface of the planet and the magnetopause boundary is devoid of any significant electrical currents except for the neutral sheet in the tail. This permits the use of a scalar potential to define the magnetic field in this source free region. By using the traditional spherical harmonic representations employed in geomagnetic field analyses, the magnetic field potential V is represented by the expression

$$V = a \sum_{n=1}^{\infty} \sum_{m=0}^{n} \left\{ \left(\frac{a}{r}\right)^{n+1} [g_n^m \cos m\phi + h_n^m \sin m\phi] + \left(\frac{r}{a}\right)^{n} [G_n^m \cos m\phi + H_n^m \sin m\phi] \right\} P_n^m (\cos \theta)$$

and $\mathbf{B} = -\nabla V$. Here g_n^m and h_n^m represent internal sources, H_n^m and G_n^m represent external sources, and a is the radius of the planet. Note that here θ is measured from the pole of the coordinate system (the $+Z$ axis) and not the equator, as is the case in the presentation of field data in this paper.

Since the data are available only in a very limited region of space along the spacecraft trajectory and indeed since the quiet magnetosphere exists for only one half of the spacecraft residence time within the magnetosphere, it is not reasonable to expect to be able to determine harmonic coefficients of high degree in any such analysis.

The approach used has been to assume internal sources described by terms of degree $n = 1$, which means a centered magnetic dipole. Even if the planet possesses an offset dipole, the $n = 1$ coefficients would be unchanged, but terms of degree $n = 2$ and greater would appear. The external sources of the field are assumed to be adequately represented by harmonics up to and including degree $n = 2$. A uniform external field is represented by the terms corresponding to $n = 1$. A least squares fit has been made to the data by using different sets of contiguous data points within the quiet interval; note that the data points used in this analysis were 42-s averages. When the data points within the magnetosphere were identified in ascending numerical order from 1 to 25, it was found that use of data points 4–13 gives results which are quite representative of the entire quiet data set, represented by data points 1–13.

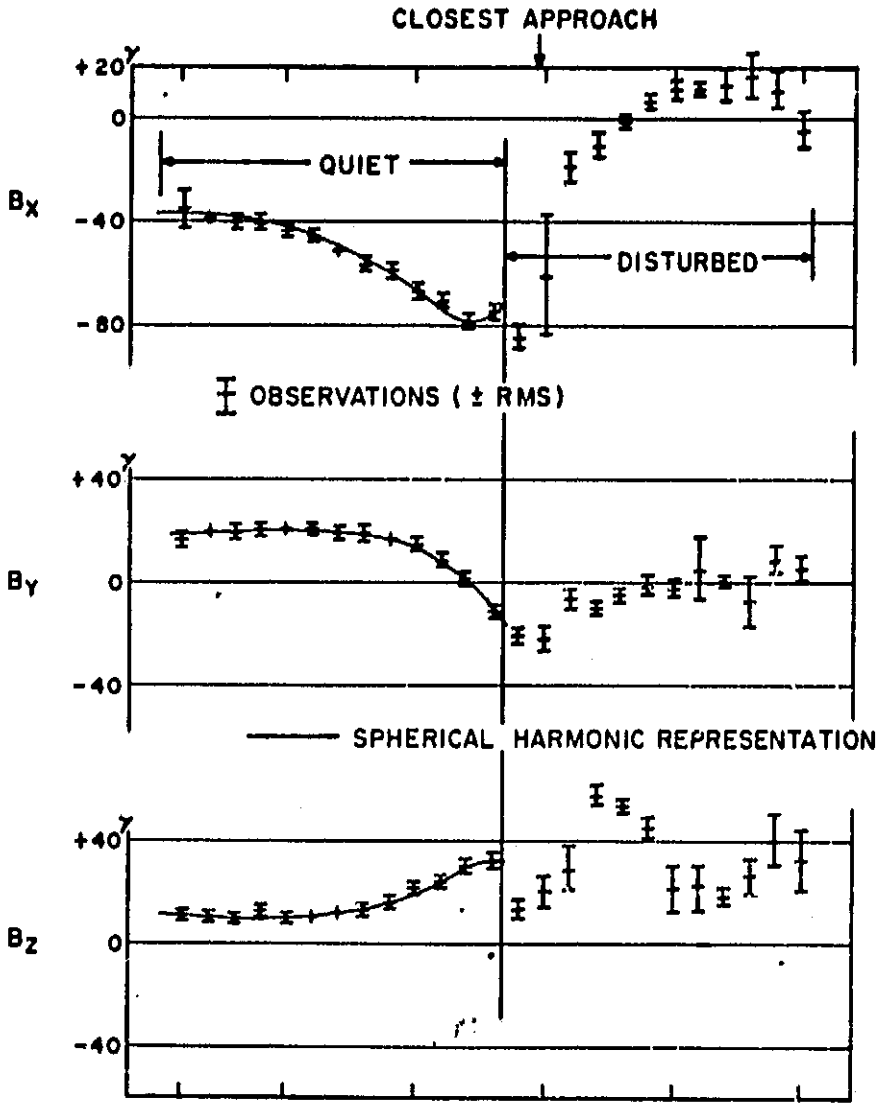

Fig. 4. Three components of magnetic field data, during Hermean magnetosphere transit, represented by 42-s averages and a least squares fit of a spherical harmonic representation, yielding a coefficient set describing the 'quiet' interval with an rms = 0.95 γ.

The least squares fit to the three orthogonal components is accomplished by a classical minimization process for the Pythagorean mean of the field components. That is, a minimum of $\sum(B_{obs} - B_{th})\cdot(B_{obs} - B_{th})$ is sought. The results obtained for the internal dipole coefficients are as follows: $g_1^0 = -344$, $g_1^1 = +16$, $h_1^1 = -59$. The fit to the data points (rms = 1 γ) is illustrated graphically in Figure 4. Here it is seen that the spherical harmonic representation fits the data very well during the quiet period of magnetosphere traversal. Another combination of harmonic coefficients has been investigated, which assumed a higher degree of complexity of the internal planetary field (i.e., $n_{int} \leq 2$) and a reduced complexity of the external field (i.e., $n_{ext} = 1$). The results so obtained were rather sensitive to the specific set of data points used, which suggested a less physically plausible representation.

From the above harmonic coefficient set it is found that the intrinsic field of the planet is represented as being due to a centered dipole of moment 5.1×10^{22} G cm³ oriented at a solar ecliptic latitude of −80° and longitude of +285°. This moment compares very well with that deduced from the positions of the magnetopause and bow shock boundaries and the inferred magnetic moment responsible for solar wind deflection. The orientation is approximately the same, but the magnitude is rather larger than that of the offset dipole obtained in the preliminary analysis. The discrepancy in dipole magnitude and location is easily understood in terms of the significant contributions of external sources, which were given no representation in the preliminary undistorted dipole field model.

It is not to be expected that the above harmonic representation of the magnetic field is valid throughout the entire Hermean magnetosphere. Rather it should be clear that the representation is constrained to the vicinity of the spacecraft trajectory. On the other hand, the internal magnetic field of the planet can be extrapolated to permit computation of the magnetic field perturbations associated with the solar wind interaction and the magnetosphere temporal disturbance.

These magnetic field perturbation vectors are presented in Figure 5, having the same format as that used in Figure 2. The characteristics of the perturbation field are clearly illustrated for both the quiet period in the magnetosphere and the disturbed period. Note that the perturbation magnetic field, when viewed from the sun, is always pointed 'southward'

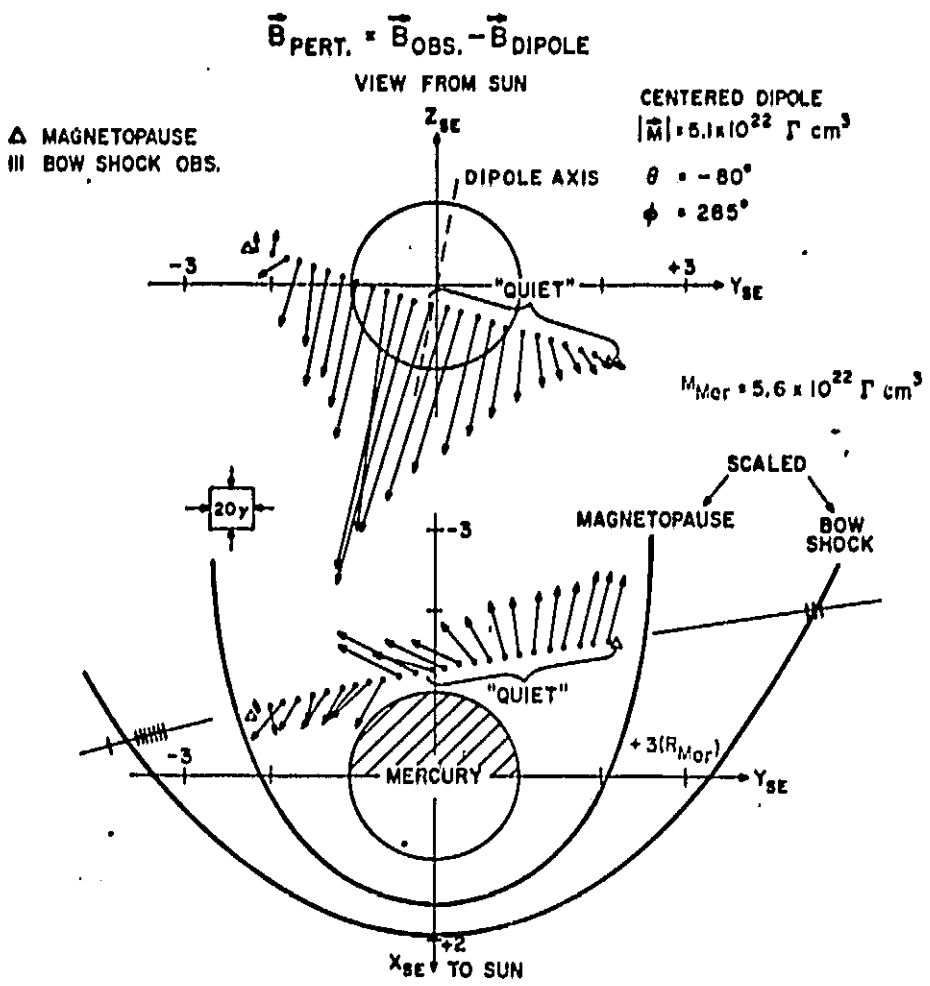

Fig. 5. Perturbation magnetic field (observed field minus internal dipole field) due to external sources, superimposed on trajectory of Mariner 10 in X-Z (top) and XY (bottom) planes during transit of Hermean magnetosphere. See Figure 2 for comparison with observed field.

throughout the entire trajectory passage through the magnetosphere. In the lower portion of the figure the sense of the perturbation field is initially antisolar just following the inbound magnetopause crossing but then swings around until, simultaneous with the disturbance of the magnetosphere, it becomes solar-directed.

In comparing this perturbation field with models of the disturbed geomagnetic field due to solar wind interaction (see Figure 3) one is compelled to draw an analogy with the existence of a neutral sheet on the dark side of Mercury due to the formation of a magnetic tail as the solar wind interacts with the planet. The spacecraft trajectory was such that Mariner 10 entered the magnetosphere below the neutral sheet and was in close proximity to it at closest approach. Thereafter, the spatial position of the spacecraft and temporal changes of the magnetosphere combined to place Mariner 10 above the extrapolated position of the neutral sheet as it exited the magnetosphere. The abrupt decrease and recovery from 2047 to 2048 UT seen in Figure 1 may be due to an intensification of the neutral sheet current as the tail field increases and/or to a motion of the edge of the neutral sheet closer to the planet.

It should be remarked that the above analysis and interpretation lead to a situation wherein the perturbation magnetic field is a large fraction of the inferred intrinsic field of the planet. For example, at the last data point in the quiet interval the Z component of the perturbation field is -109 γ, which is 80% of the dipole field, $+140$ γ. Its polarity is opposite to the internal field, and this is consistent with the fact that the general topology of the magnetic field of the magnetosphere of Mercury is similar to that of the earth.

Implications

The existence of both a modest magnetic field of Mercury sufficient to deflect the solar wind and an imbedded neutral sheet leads to the conclusion that there should exist a magnetic tail of Mercury. The possible characteristics of such a magnetic tail are illustrated in Figure 6. Assuming that the magnetic flux in the polar regions of the planet connect with the tail and that negligible merging takes place across the neutral sheet, one can infer the size of the polar cap region.

Measurements of the magnetic field just after the inbound magnetopause crossing suggest that for Mercury the tail field is 30–40 γ with a radius of approximately 2.0 to 2.6 R_{Mer}. With the assumed magnetic dipole moment of 5.1×10^{22} G cm³ for the planet, this leads to a polar cap colatitude of

18–26°, approximately twice that of the earth's polar cap colatitude.

The optical properties of the Hermean surface are similar in many respects to those of the moon [*Hameen-Anttila et al.*, 1970; *McCord and Adams*, 1972]. The lunar surface optical properties are influenced most by size, composition, and structure but also by ion bombardment by the solar wind. It is believed that the flux of solar wind ions impacting the lunar surface leads to a darkening of surficial material [*Hapke*, 1971]. With this point in mind, it becomes then necessary to investigate whether or not the magnetic field inferred for Mercury is such that it would always deflect the solar wind flow from the planetary surface.

The preliminary interpretation of a tilted dipole with appreciable offset led naturally to a situation in which the solar wind periodically could impact the surface during each planetary orbit. The present interpretation, using a centered dipole, yields a value of magnetic dipole which is sufficient to deflect the solar wind momentum flux at most times during the planetary orbit except those when the solar wind flux is higher than average when the planet is near perihelion.

Figure 7 illustrates the relationship between solar wind momentum flux, equatorial field strength B_0, and radius of the subsolar magnetopause R_{mp}, in units of planetary radius R_p. It has already been deduced [*Ness et al.*, 1974*b*] that at the first

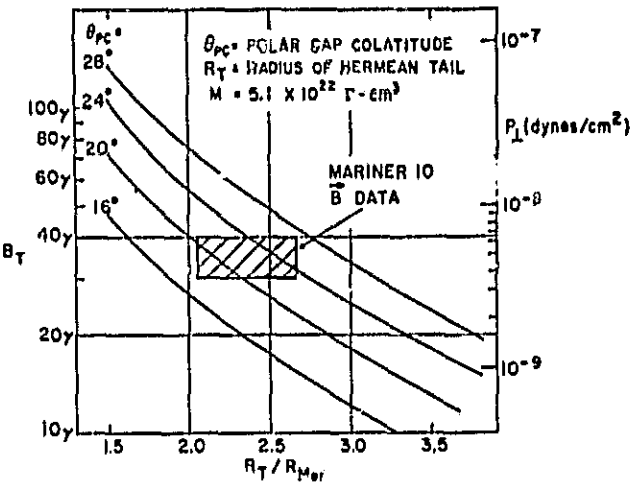

Fig. 6. Relationship of magnetic tail field intensity B_T to radius of tail R_T as function of polar cap colatitude; the centered internal dipole moment is assumed to be 5.1 × 10²² G cm³.

Mercury encounter the solar wind momentum flux of 1.1 × 10^{-7} dyn/cm (±10%) and the inferred standoff distance of 1.6 R_p lead to an intrinsic equatorial field strength of 380 ± 32 γ. If the solar wind momentum flux increases by a factor of 5, then the magnetopause is pushed down to $1.2R_{Mer}$, which is

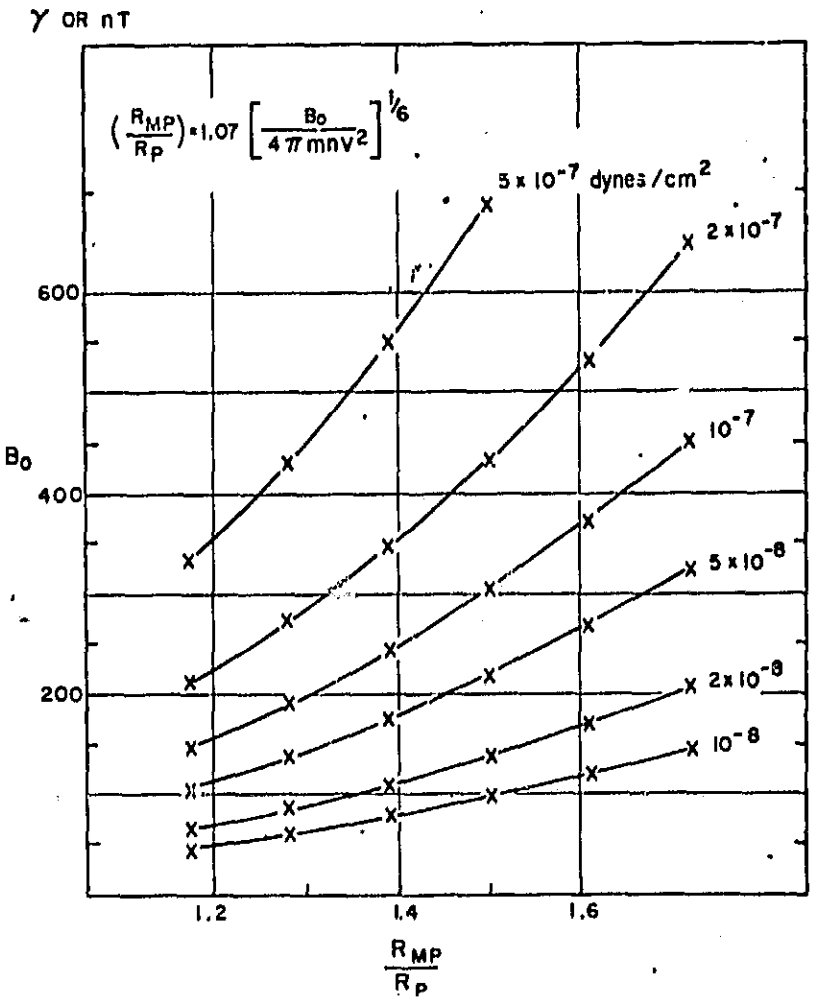

Fig. 7. Relationship between equatorial field strength B_0 (for a planetary field modeled by a magnetic dipole perpendicular to solar wind velocity) and distance to stagnation point R_{mp}, normalized in planetary radius R_p for various values of deflected solar wind momentum flux mnV^2. Theoretical relationship given by *Choe et al.* [1973].

less than 500 km above the surface. On this scale the fluid approximation to solar wind flow begins to break down because of the finite size of the cyclotron radius, 50–100 km, and the finite thickness of the magnetopause. A further increase in solar wind flux leads to a situation wherein the solar wind ions approach within 1 gyroradius of the planetary surface, so that the deflection of the flow would be incomplete as the solar wind begins to impact directly and to be absorbed by the planetary surface. It should be noted that in analogy with the earth, solar wind and more energetic particles have direct access to the planet through the polar cap and neutral sheet.

Summary and Conclusions

An improved quantitative analysis of the magnetic field data obtained by Mariner 10 during the first Mercury encounter on March 29, 1974, is presented. The limited data available during the time interval when the magnetospherelike region was in a steady state condition restrict the ability to evaluate the nature of the planetary field uniquely. By assuming a centered magnetic dipole for the intrinsic field of the planet and by attributing the distortion of the dipole field to fields associated with external sources whose complexity is well represented by harmonics up to degree 2, a least squares analysis yields an excellent fit (rms = 0.95 γ) and a very self-consistent interpretation to the composite data set.

The intrinsic magnetic field dipole moment is found to be 5.1×10^{22} G cm^3, oriented in a polarity sense similar to earth's dipole and at solar ecliptic $\theta = -80°$ and $\phi = 285°$. Subtracting this intrinsic field from the observed field yields a perturbation field, due to magnetopause and magnetotail currents, whose characteristics are similar to the spatial and also the temporal distortion of the magnetosphere as in the earth's case. The dipole axis is tilted only 7.2° from the normal to Mercury's orbital plane and is thus within 4°–10° of the rotation axis.

A fundamental question which is unresolved is that of the origin of this global intrinsic planetary field. At the present time we do not believe that the data support theories invoking a complex induction source mechanism due to the flow of the solar wind. Two possible alternatives are a present day active dynamo or fossil magnetization due to an ancient dynamo or an enhanced interplanetary magnetic field during cooling. Both depend upon the thermal state of the planetary interior, and it is not possible to distinguish between the two mechanisms. Partially, this is due to our lack of a precise model for a planetary dynamo [*Gubbins*, 1974] and also to the lack of information concerning the structure of the planetary interior. Due to the high average density of the planet, 5.44 g/cm^3, it is fairly certain that a large amount of iron exists, on the order of 60%, which is probably concentrated in a large core [*Kozlovskaya*, 1969; *Plagemann*, 1965; *Reynolds and Summers*, 1969; *Siegfried and Solomon*, 1974; *Toksoz and Johnston*, 1975]. If such a core were at low temperatures, below the Curie point, then a remanent magnetic field is quite plausible, although then the problem is to determine the origin of the magnetizing field.

The possibility of a sufficiently cold core seems very remote in the light of studies on the thermal evolution of the terrestrial planets. *Toksoz and Johnston* [1975] have shown that early in Mercury's history a substantial iron nickel core formed with a radius of approximately 1600 km. Such a large core can probably support a planetary dynamo, if the appropriate combination of fluid motions and electrical properties exists. While the slow rotation of the planet may appear to be an impediment to the successful application of dynamo theory, the important physical parameters for a dynamo include dimensionless numbers for flattening, the differential rotation of the planetary interior, the magnetic Reynolds number, and other such quantities. We do not believe that sufficient data exist at present to uniquely exclude an active dynamo from further consideration for the origin of the magnetic field. It does appear doubtful that the decay of an ancient dynamo could have a time constant long enough to sustain the field, based on any reasonable estimate of core electrical conductivity and magnetic permeability.

With a warm or hot interior the question arises as to whether or not fossil magnetization of a thin solid mantle would be possible. Again the absence of definitive information on the thermal characteristics of near-surface material precludes an answer to this question. However, it is instructive to consider the magnitude of remanent magnetization required, in spite of the probable high near-surface temperatures. When a uniformly magnetized thin spherical shell is assumed, the magnetization required is not much larger than the remanent magnetizations found in the returned lunar samples [*Fuller*, 1974]. With a lithospheric shell below the Curie point whose thickness is 20% of the radius, 488 km, the necessary magnetization is 3.1×10^{-4} emu/g. For 10%, 244 km, the value rises to 5.9×10^{-4} emu/g. This is well within the range of materials which may be expected to be present on the planet Mercury, since lunar surface materials yield magnetizations generally within an order of magnitude of 10^{-3} emu/g but at much lower temperatures.

In the light of the limited data set available it is not uniquely possible to choose between these two sources of magnetic field: active dynamo or fossil magnetism. As yet there is no agreement on whether the thermal history of Mercury includes the evolution of a fluid core [*Majeva*, 1969; *Plagemann*, 1965; *Siegfried and Solomon*, 1974] or whether there exists a lithospheric shell whose temperatures are below the Curie point. Perhaps additional data obtained during the third Mercury encounter on March 16, 1975, will illuminate more clearly the quantitative characteristics of the planetary field, and hence its origin.

Acknowledgments. We appreciate the efforts of Richard Thompson of GSFC in the analysis of the data.

The Editor thanks D. Beard and G. L. Siscoe for their assistance in evaluating this paper.

References

Bridge, H. S., A. J. Lazarus, J. D. Scudder, K. W. Ogilvie, R. E. Hartle, J. R. Asbridge, S. J. Bame, W. C. Feldman, and G. L. Siscoe, Observations at Venus encounter by the plasma science experiment on Mariner 10, *Science, 183*, 1293, 1974.

Broadfoot, A. L., S. Kumar, M. J. S. Belton, and M. B. McElroy, Mercury's atmosphere from Mariner 10: Preliminary results, *Science, 185*, 166, 1974.

Choe, J. T., D. B. Beard, and E. E. Sullivan, Precise calculation of the magnetosphere surface for a tilted dipole, *Planet. Space Sci., 21*, 485, 1973.

Fuller, M., Lunar magnetism, *Rev. Geophys. Space Phys., 12*, 23, 1974.

Gubbins, D., Theories of the geomagnetic and solar dynamos, *Rev. Geophys. Space Phys., 12*, 137, 1974.

Hameen-Anttila, K. A., T. Pikkarainen, and H. Camichel, Photometric studies of the planet Mercury, *Moon, 1*, 440, 1970.

Hapke, B., Optical properties of the lunar surface, in *Physics and Astronomy of the Moon*, edited by Z. Kopal, 2nd ed., p. 155, Academic, New York, 1971.

Howard, H. T., et al., Mercury: Results on mass, radius, ionosphere and atmosphere from Mariner 10 dual frequency radio signals, *Science, 185*, 179–180, 1974.

Kozlovskaya, S. V., On the internal constitution and chemical composition of Mercury, *Astrophys. Lett.*, *4*, 1, 1969.
Majeva, S. V., The thermal history of the terrestrial planets, *Astrophys. Lett.*, *4*, 11, 1969.
McCord, T. B., and J. B. Adams, Mercury: Interpretation of optical observations, *Icarus*, *17*, 585–588, 1972.
Ness, N. F., K. W. Behannon, R. P. Lepping, Y. C. Whang, and K. H. Schatten, Magnetic field observations near Venus: Preliminary results from Mariner 10, *Science*, *183*, 1301, 1974*a*.
Ness, N. F., K. W. Behannon, R. P. Lepping, Y. C. Whang, and K. H. Schatten, Magnetic field observations near Mercury: Preliminary results, *Science*, *185*, 151, 1974*b*.
Ogilvie, K. W., J. D. Scudder, R. E. Hartle, G. L. Siscoe, H. S. Bridge, A. J. Lazarus, J. R. Asbridge, S. J. Bame, and C. M. Yeates, Observations at Mercury encounter by the plasma science experiment on Mariner 10, *Science*, *185*, 145, 1974
Plagemann, S., A model of the internal constitution and temperature of the planet Mercury, *J. Geophys. Res.*, *70*, 985, 1965.
Reynolds, R., and A. Summers, Calculations on the composition of the terrestrial planets, *J. Geophys. Res.*, *74*, 2494–2511, 1969.
Siegfried, R. W., and S. C. Solomon, Mercury: Internal structure and thermal evolution, *Icarus*, *23*, 192, 1974.
Simpson, J. A., J. H. Fraker, J. E. Lamport, and P. H. Walpole, Electrons and protons accelerated in Mercury's magnetic field, *Science*, *185*, 160, 1974.
Siscoe, G., N. F. Ness, and C. M. Yeates, Substorms on Mercury?, *Geophys. Res. Lett.*, in press, 1975.
Stevenson, D., Planetary magnetism, *Icarus*, *22*, 403, 1974.
Toksoz, M. N., and D. H. Johnston, The evolution of the moon and the terrestrial planets, in *Proceedings of the Soviet-American Conference on the Moon and Planets*, in press, 1975.

(Received December 12, 1974;
accepted February 21, 1974.)